467 Gbit/s Net Bitrate IM/DD Transmission Using 176 GBd PAM-8 Enabled by SiGe AMUX with Excellent Linearity

Qian Hu[1], Tobias Tannert[2], Markus Grözing[2], Gregory Raybon[1], Robert Borkowski[1], Fred Buchali[3], Xi Chen[1], Pat Iannone[1], Georg Rademacher[2], Roland Ryf[1]

[1] Nokia Bell Labs, 600 Mountain Ave, Murray Hill, NJ 07974, USA
[2] University of Stuttgart, INT, Pfaffenwaldring 47, 70569 Stuttgart, Germany
[3] Nokia, Network Infrastructure – Optical Networks, Magirusstr. 8, 70469 Stuttgart, Germany
qian.hu@nokia-bell-labs.com

Abstract: Using a SiGe analog multiplexer (AMUX) integrated circuit we generate a PAM-8 signal at 176 GBd by time-interleaving two 88 GBd tributaries. High-quality signal is obtained after interleaving thanks to the excellent linearity of the AMUX. We successfully demonstrate net bitrates up to 467 Gbit/s after 2 km fiber transmission.

1. Introduction

An N:1 analog multiplexer (AMUX) operates as a high-speed switch which interleaves waveforms from *N* parallel digital-to-analog converters (DACs) in time domain. Such circuits are of particular interest and importance for next generation short- and long-reach optical transmission systems, where expected symbol rates can hardly be supported by direct signal generation using CMOS DACs. Use of an AMUX integrated circuit (IC) built in a broadband technology (e.g., silicon germanium, SiGe, or indium phosphide, InP) can result in a significant increase of analog bandwidth and sampling rate. Moreover, AMUX circuits can be monolithically integrated with drivers in the same technology, thus do not further increase transmitter component count and do not add new integration complexity. The analog bandwidth, the switching speed, and the linearity of the AMUX are the most important design criteria for applications targeting transmission using high-order modulation formats at ultrahigh symbol rates. In recent years, several high-speed optical transmission experiments have been reported using AMUX ICs implemented in InP [1–9] as well as SiGe [10–12] processes. Fig. 1(a) provides an overview of the achieved net bitrates in a function of symbol rate for system experiments involving time-interleaving AMUXes. For coherent transmission experiments (hollow markers), net bitrate per one quadrature (dimension) is used for fair comparison. The advantages of the SiGe technology in terms of yield, cost and availability makes it an attractive platform. The SiGe AMUX IC tested in this paper was manufactured in the 130 nm technology SG13G3 of IHP, providing heterojunction bipolar transistors with f_T = 500 GHz and f_{max} = 700 GHz [13]. The circuit topology and design details can be found in [14]. In a previous experiment [15], this type of AMUX IC was used to generate electrical 4-level pulse amplitude modulation (PAM-4) signals up to 190 GBd in an electrical back-to-back measurement.

The broadband 2:1 SiGe AMUX IC under test is characterized by excellent linearity of the multiplexing process, allowing for generation of high-order modulation formats. Using the AMUX IC, we experimentally demonstrate 176 GBd optical PAM-8 transmission over a 2 km fiber, achieving a net bit rate of 467 Gbit/s. To the best knowledge of the authors, this is the highest net bitrate in a single modulation dimension demonstrated using AMUX IC.

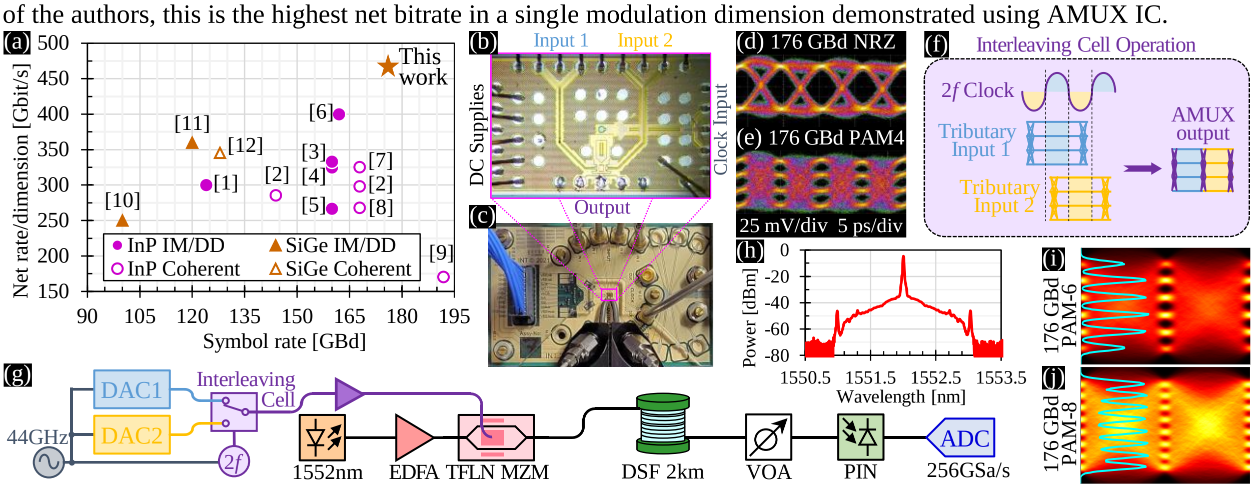

Fig. 1. (a) Overview of the reported time-interleaving AMUX-based experiments. Photos of: (b) AMUX chip and (c) evaluation board. Electrical eye diagrams of 176 GBd signals: (d) NRZ and (e) PAM-4. (f) Illustration of switching operation in the AMUX interleaving cell. (g) Experimental setup. (h) Optical spectrum. Eye diagrams of equalized 176 GBd signals: (i) PAM-6, (j) PAM-8.

2. Experimental Setup and DSP

Figure 1 shows photographs of: (b) the AMUX IC tested in this work, and (c) the evaluation board (EVB) housing the chip. The IC is glued inside a slot in the center of the EVB. The data, clock and DC inputs of the chip are wire-bonded to the EVB, which has GPPO connectors for differential data and clock inputs and a multi-pin connector for DC supplies. The AMUX differential outputs are probed with a 110 GHz RF probe. Fig. 1(f) provides an illustration of the switching operation in the interleaving cell of the 2:1 AMUX IC. During each half cycle of the clock signal, the data signal from one input path is switched to the common output, while the data signal from the other input path is switched to a dummy path. Thus, the signal formed at the output of the interleaving cell has double the symbol rate of the input data. A clock multiplier with an input frequency range from 43 GHz to 44 GHz is integrated on the AMUX chip. As shown in the experimental setup in Fig. 1(g), a 44 GHz clock signal is provided to two parallel DACs and the AMUX, which is internally doubled to 88 GHz after the clock multiplier, resulting in 176 GSa/s operation of the interleaving cell. With a different design of the clock multiplier, the interleaving cell can support higher sampling rates. The two individual DACs generate two 88 GBd PAM tributary signals and thus a 176 GBd interleaved PAM signal is obtained at the output of the AMUX. Figs. 1(d,e) show eye diagrams recorded single-ended at one of the AMUX differential outputs. An SNR as high as 21 dB is achieved. The eye diagram of the PAM-4 signal demonstrates the excellent linearity of the circuit, which is required to support interleaving of high-order modulation formats.

The remaining part of the experimental setup is shown in Fig. 1(g). The optical intensity-modulated signal is generated by modulating the output of a 1552 nm external cavity laser in a thin-film lithium-niobate Mach-Zehnder modulator (MZM) with V_π=2.6 V and ≈70 GHz 3-dB electro-optic bandwidth. The MZM has a high insertion loss (IL) of 12 dB, attributed mainly to the optical input and output grating couplers, accounting for approximately 9 dB excess loss. To compensate for the high MZM IL, an erbium-doped fiber amplifier is used to increase the optical power at the input of the MZM to 25 dBm. The electrical signal from the AMUX is first amplified by a 100 GHz driver amplifier and provided to the modulator. The MZM is biased slightly below the quadrature point to improve the extinction ratio. The optical signal at the MZM output having 9 dBm optical power is launched into a 2 km dispersion shifted fiber (DSF) with zero dispersion wavelength at 1551.9 nm. The DSF is used to avoid severe penalties due to power fading of broadband signals induced by fiber chromatic dispersion. At the receiver side, a variable optical attenuator (VOA) is used to control the optical power entering a 100 GHz PIN photodetector, which is directly connected to a 256 GSa/s oscilloscope with 113 GHz analog bandwidth.

The frequency response of the AMUX setup, including the AMUX IC and two DACs is calibrated in an electrical back-to-back (B2B) configuration, from which a digital pre-emphasis filter is derived. In the transmitter DSP, we deliberately reduce peaking of the pre-emphasis filter to increase electrical signal amplitude, which is the most important factor limiting performance in this experiment. The pre-emphasized signal is digitally deinterleaved to form two tributaries for generation by two 88 GSa/s DACs at 1 Sa/symbol (Sps). Fig. 1(h) shows the resulting optical spectrum at the transmitter output. The tones appearing outside the signal spectrum at 132 GHz are due to mixing of 44 GHz and 88 GHz clock signals in the integrated clock multiplier.

In the offline receiver DSP, the digitized signal is resampled to 2 Sps. An equalizer structure optimized for time-interleaved signal is used: two copies of the signal are fed into two T/2-spaced feedforward equalizers (FFEs), where one FFE produces odd symbols, while the other FFE produces even symbols. Such equalizer structure is employed considering the different signal distortions occurring in the two signal tributary paths before the interleaving cell. Each FFE contains 129 linear term taps, 15 second-order term taps (x_k^2 and $x_k x_{k-1}$) and 15 third-order term taps (x_k^3), where x_k represent signal sample at instance k. The second- and third-order terms are used mainly to compensate for the nonlinear transfer function of the MZM and can be omitted with small performance degradation. A decision feedback equalizer with 5 taps is also used. Finally, bit error ratio (BER) is counted and normalized generalized mutual information (NGMI) metric is computed.

3. Results

Transmission performance is measured for PAM signals with 2, 3, 4, 6 or 8 amplitude levels. For PAM-3/-6 signal, two-dimensional modulation is used. Both quadratures of a QAM-8/-32 signal are interleaved in consecutive time slots [16]. Fig. 2(a) shows BERs measured for all modulation formats as a function of received optical power in optical B2B configuration and after 2 km fiber transmission, which closely overlap. At the highest received optical power after fiber transmission (6.6 dBm), a BER of 1.74×10^{-2} is obtained with PAM-8, which is below the BER threshold required for 25% overhead (1.82×10^{-2} at code rate 0.8) hard-decision forward error correction (HD-FEC) based on staircase codes [17]. The BER decreases to 2.24×10^{-3} using PAM-6, which is below the threshold for 6.25% overhead (4.7×10^{-3} at code rate 0.9412). The BER is 1.35×10^{-5} when using PAM-4, and no errors are measured for PAM-3 and

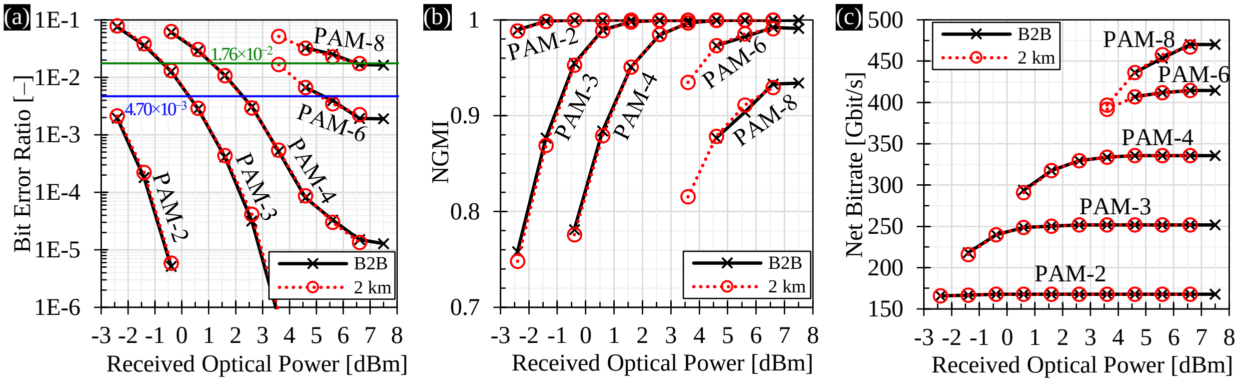

Fig. 2. Experiment results. (a) Bit error ratio as a function of the received optical power for different PAM orders, back-to-back (solid black lines with ×) and after fiber (dotted red lines with ○). (b-c) NGMI and corresponding net bitrate as a function of the received optical power for different PAM orders.

PAM-2. Figs. 1(i) and (j) show eye diagrams of 176 GBd PAM-8 and PAM-6 signals at the highest received optical power after equalization. SNR of 18.8 dB is achieved.

NGMI is computed for all measured signals and plotted in Fig. 2(b). At the highest received optical power after fiber transmission, NGMI values of 0.9296 and 0.9907 are achieved with PAM-8 and PAM-6 signals, respectively. The NGMI values are above 0.9990 for PAM-2/-3/-4 signal. While the NGMI values decreases with the received optical power, the decrease only becomes noticeable at received optical powers below 3.6 dBm for PAM-4, 1.6 dBm for PAM-3 and −1.4 dBm for PAM-2. The net bitrates are computed by mapping the NGMI results in Fig. 2(b) onto the NGMI thresholds in [16] for soft-decision and hard-decision concatenated FEC coding. The mapped NGMI thresholds lead to net bitrates of $r_c R_s H$, where r_c is the FEC code rate corresponding to the NGMI threshold, R_s is the symbol rate and H is the entropy of the applied modulation format. H equals to 1/1.5/2/2.5/3 bit/symbol for PAM-2/-3/-4/-6/-8 signal. The obtained net bitrates are plotted in Fig. 2(c). With PAM-6 and PAM-8 signals, a net bitrate above 400 Gbit/s can be achieved when the received optical power is equal to or higher than 4.6 dBm. At the highest received optical power after fiber transmission, a net bitrate of 414.5 Gbit/s is achieved with PAM-6 signal, 467.1 Gbit/s with PAM-8.

4. Conclusions

We successfully demonstrate generation, transmission, and reception of 176 GBd intensity-modulated PAM signals with up to 8 amplitude levels created by analog interleaving of two PAM tributaries at 88 GBd using a SiGe analog multiplexer (AMUX) integrated circuit (IC). Measurements demonstrate the broad analog bandwidth and the excellent linearity of the AMUX IC, which has great potential to support the growth of data rates in future optical transmission systems. With a 176 GBd PAM-6 signal, net bitrates (post-FEC) above 400 Gbit/s can be achieved after transmission over a 2 km fiber at a received optical power equal to or higher than 4.6 dBm. With a 176 GBd PAM-8 signal, a net bitrate of 467.1 Gbit/s is achieved at 6.6 dBm received optical power.

5. References

[1] H. Yamazaki *et al.*, "300 Gbps discrete multi-tone transmission using digital-preprocessed analog-multiplexed…," ECOC 2016, pp. 1–3.
[2] F. Hamaoka *et al.*, "144-Gbaud PDM-32QAM and 168-Gbaud PDM-16QAM signal generation using ultra- …," Proc. ECOC 2019, pp. 445–447.
[3] H. Yamazaki *et al.*, "IMDD transmission at net data rate of 333 Gb/s using over-100-GHz-bandwidth…," JLT **37**, 1772–1778 (2019).
[4] N. P. Diamantopoulos *et al.*, "Net 321.24-Gb/s IMDD transmission based on a >100-GHz bandwidth directly-…, OFC 2020, p. Th4C.1.
[5] H. Yamazaki *et al.*, "160-GBd (320-Gb/s) PAM4 transmission using 97 GHz bandwidth analog multiplexer," PTL **30**, 1749–1751 (2018).
[6] H. Yamazaki *et al.*, "Net 400 Gbps PS-PAM transmission using integrated AMUX-MZM," Opt. Express **27**, 25544–25550 (2019).
[7] M. Nakamura *et al.*, "1.3 Tbps/carrier net-rate signal transmission with 168 GBaud PDM PS-64QAM using…," Proc. ECOC 2019, pp. 409–411.
[8] M. Nagatani *et al.*, "A 110-GHz-bandwidth 2:1 AMUX-driver using 250-nm InP DHBTs for beyond-1-Tb/s/ …," BCICTS 2019, pp. 1–4.
[9] M. Nakamura *et al.*, "192-Gbaud signal generation using ultra-broadband optical frontend module integrated with…," OFC 2019, Th4B.4.
[10] K. Schuh *et al.*, "100 GSa/s BiCMOS analog multiplexer based 100 GBd PAM transmission over 20 km single-…," ECOC 2020, p. Tu1E.4.
[11] Q. Hu *et al.*, "120 GSa/s BiCMOS analog multiplexer enabling 360 Gbit/s DSCM-PCS-256QAM IM/DD transmission," OFC 2021, p. F2D.1.
[12] Q. Hu *et al.*, "128 GSa/s SiGe analog multiplexer enabling PDM-DSCM-PCS-256QAM transmission over 80 km SSMF," APC 2022, p. SpTh1I.6.
[13] B. Heinemann *et al.*, "SiGe HBT with f_T/f_{max} of 505 GHz/720 GHz, " Proc. IEDM 2016, pp. 51–54.
[14] T. Tannert *et al.*, "Analog 2:1 Multiplexer with over 110 GHz Bandwidth in SiGe BiCMOS Technology," BCICTS 2021, p. 5a.3.
[15] J. Schostak *et al.*, "190 GBd PAM-4 Signal Generation using Analog Multiplexer IC with On-Chip Clock Multiplier," Proc. EuMIC 2023, pp. 125–128.
[16] Q. Hu *et al.*, "Ultrahigh-net-bitrate 363 Gbit/s PAM-8 and 279 Gbit/s polybinary optical transmission…," JLT **40**, 3338–3346 (2022).
[17] L. M. Zhang and F. R. Kschischang, "Staircase codes with 6% to 33% overhead," JLT **32**, 1999–2002 (2014).